CrossMark

Effects of Carbon Allotropic Forms on Microstructure and Thermal Properties of Cu-C Composites Produced by SPS

K. Pietrzak, N. Sobczak, M. Chmielewski, M. Homa, A. Gazda, R. Zybała, and A. Strojny-Nędza

Combination of extreme service conditions and complex thermomechanical loadings, e.g., in electronics or power industry, requires using advanced materials with unique properties. Dissipation of heat generated during the operation of high-power electronic elements is crucial from the point of view of their efficiency. Good cooling conditions can be guaranteed, for instance, with materials of very high thermal conductivity and low thermal expansion coefficient, and by designing the heat dissipation system in an accurate manner. Conventional materials such as silver, copper, or their alloys, often fail to meet such severe requirements. This paper discusses the results of investigations connected with Cu-C (multiwall carbon nanotubes (MWNTs), graphene nanopowder (GNP), or thermally reduced graphene oxide (RGO)) composites, produced using the spark plasma sintering technique. The obtained composites are characterized by uniform distribution of a carbon phase and high relative density. Compared with pure copper, developed materials are characterized by similar thermal conductivity and much lower values of thermal expansion coefficient. The most promising materials to use as heat dissipation elements seems to be copper-based composites reinforced by carbon nanotubes (CNTs) and GNP.

1. Introduction

The continuous progress in electronics industry leads to increased requirements for heat sink materials. Dissipation of heat generated in electronic high-power components (e.g., diodes, thyristors, and lasers) during their operation has crucial significance for their effectiveness. Heat flux density during the operation of, e.g., semiconductor lasers may even amount to 10 kW/cm^2 (Ref [1]). Favorable cooling conditions can be achieved by, e.g., designing the heat-dissipating system and using appropriate advanced materials. The materials intended to be used in electronics should be characterized by the following features: the heat conductance comparable with that of copper (250-400 W/mK), the thermal expansion coefficient matched with the properties of semiconductor materials (Si, GaAs—3.0-6.0 × 10^{-6} 1/K), advantageous mechanical properties such as the Young modulus > 140 MPa, good machinability, ability to

form durable joints, stability of the structure during thermal cycles (within the specified temperature range dependent on a given application), low cost comparable to that of other materials competitive with them, and, last but not the least, the possibility of their recycling. As a result, the proper choice of the used materials and technological process of their preparation are getting more and more important.

The fulfillment of these requirements by the conventional materials is practically impossible. At present, many studies devoted to the design and fabrication of advanced materials, characterized by a very good thermal conductivity, such as Cu-Mo, Cu-Be, Cu-C$_F$, Cu-SiC, Cu-AlN, Al-SiC, Al-AlN, etc., are being carried out worldwide (Ref [2]-[7]). Copper with its thermal conductivity of about 400 W/mK is always used wherever high thermal and electric conductivities are required, but its application range is limited because of the unsatisfactory mechanical properties, especially at elevated temperatures. Moreover, the high thermal expansion coefficient of copper (16.5 × 10^{-6} 1/K) may result in considerable residual stresses being induced and in thermal dilatation occurring, when the copper components are subjected to substantial temperature variations.

One of the possible solutions to this problem can be the development of a new group of copper-based materials. The combination of the specific properties of copper and selected allotropic forms of carbon should result in a material with the desired properties, which could be used as a heat dissipation material. Copper-carbon composites can be produced applying a variety of processing techniques, but in all these cases, a very significant problem must be solved, i.e., the homogenous distribution of a carbon phase in a copper matrix (Ref [8]). Uniform dispersion of graphene or other nanoforms has been the main challenge in the case of this kind of metal-matrix composites (MMCs) because graphene has a well-developed specific surface area, which leads to the formation of clusters due to van der Waals forces. The modeling results in (Ref [9]) demonstrate that the thermal conductivity of the Cu-C interface

K. Pietrzak, M. Chmielewski, and A. Strojny-Nędza, Institute of Electronic Materials Technology, 133 Wolczynska Str., 01-919 Warsaw, Poland; N. Sobczak, M. Homa, and A. Gazda, Foundry Research Institute, 73 Zakopianska Str., 30-418 Kraków, Poland; and R. Zybała, Faculty of Materials Science Engineering, Warsaw University of Technology, 141 Woloska Str., 02-507 Warsaw, Poland. Contact e-mail: katarzyna.pietrzak@itme.edu.pl.

is a crucial factor and decreases with an increase in the number of graphene layers.

Various forms of carbon, in particular graphene, have generated a lot of interest due to their characteristics. Graphene is a 2D form of carbon atoms arranged in a honeycomb lattice. Apart from being 100 times stronger than steel, one atom-thick graphene is flexible, transparent, and is known to conduct heat better than silver and conduct electricity better than silicon. Its thermal conductivity (4800-5300 W/mK), which is more than twice as high as that of diamond ($\lambda = 2000$ W/mK), is the highest ever recorded (Ref [10]). In addition, due to having low electrical resistance, graphene is also an excellent electrical conductor. Carbon nanotubes (CNTs) are strong and stiff materials. CNTs can withstand pressure up to 25 GPa without deformation, and the bulk modulus of superhard phase nanotubes is up to 546 GPa (Ref [11]). Measurements show that a CNT has a room-temperature thermal conductivity of about 3500 W/m K along its axis (Ref [12]). Its temperature stability has been estimated to be up to 2800 °C in vacuum and about 750 °C in air (Ref [13]).

Composites based on copper doped with carbon (Cu-C) are claimed to combine the unusual electrical (conductivity), thermal (heat conduction), and tribological properties (low coefficient of friction). They are used in electric engine brushes, plain bearings, etc. (Ref [14], [15]).

There are a great number of manufacturing methods of Cu-C, including the following (Ref [16], [17]):

– Cu-C as a bulk material: microwave sintering, hot-pressing, spark plasma sintering (SPS), cold pressing, hot-isostatic pressing, liquid infiltration, and diffusion bonding; and
– Cu-C as layers: microwave plasma-enhanced chemical vapor deposition and tape casting.

SPS is one of the most promising techniques employed to produce composite materials (Ref [18]). In this method, the consolidation of powder material is influenced by a combination of both pressure and temperature, accompanied by the passage of an electric current. The possibility of performing a quick pressing process of various powders has to be reckoned as its predominant advantage. Arcing can appear in pores during electric current-assisted sintering, thus intensifying the sintering processes. Second, the particularly important feature of this method is that the electric current-assisted sintering of powder materials does not alter the microstructure of the sintered materials and does not cause growth of grains and their agglomeration.

The present paper shows some technological aspects of the preparation of the powder mixtures of copper and carbon nanoforms and sintering process by the SPS method. The influences of the carbon form on the microstructure and thermal properties of Cu-C composites are also presented and discussed.

2. Materials and Experimental Procedure

In this experiment, copper powder produced by Sigma Aldrich, having a dendritic shape, grain size of 3 μm, and purity of 99.8%, was used as a starting material. Three different forms of carbon (multiwall carbon nanotubes—MWNT, graphene nanopowder—GNP, or thermally reduced graphene oxide—RGO) with the volume fraction of 3% were added as a
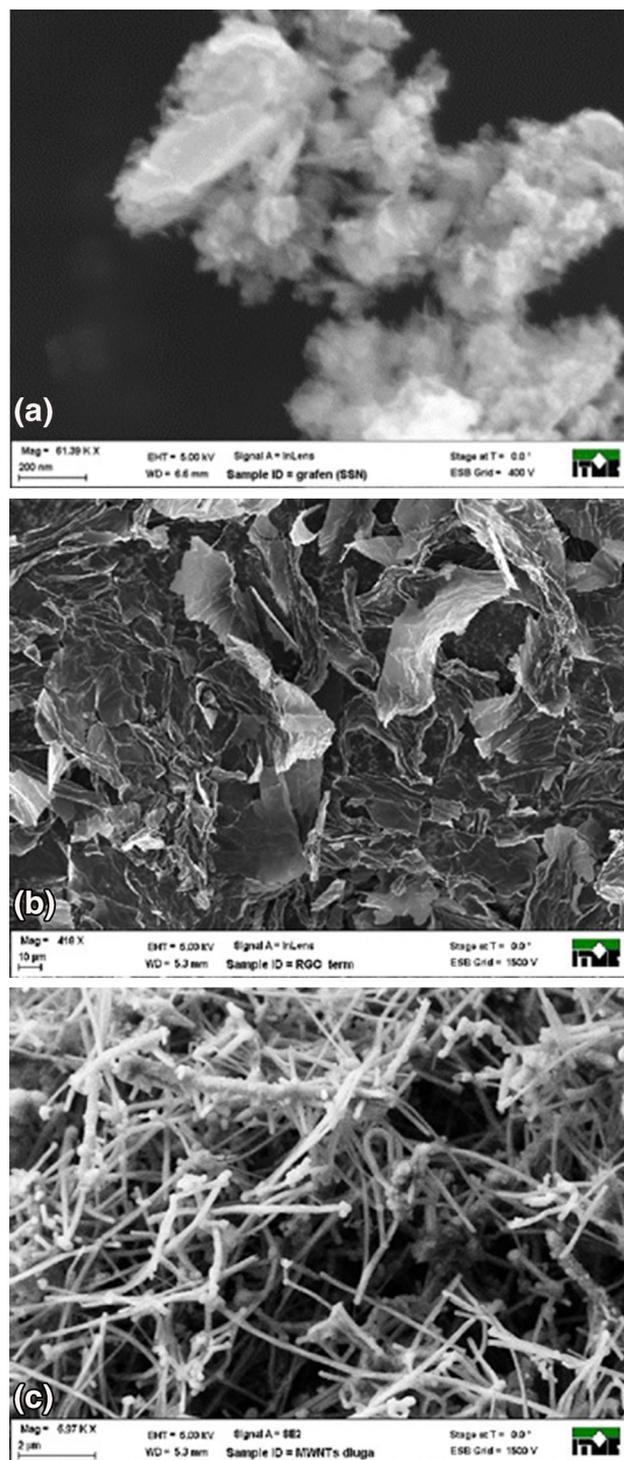

Fig. 1 SEM images of carbon nanoforms: (a) graphene nanopowder, (b) thermally reduced graphene oxide, (c) multiwall carbon nanotubes

reinforcement. Figure 1 shows the morphologies of the different carbon forms used in the experiments. The properties of the carbon forms were as follows:

• graphene nanopowder (from SkySpring Nanomaterials): particle size, between 1 and 5 μm (about 5-10 layers); specific surface area, 120-150 m^2/g; and purity 99.5%.

- thermally RGO (from ITME): size of sheets, 30 μm (30-70 layers).
- multiwall carbon nanotubes (from Sigma Aldrich): 10 walls approximately of 5-μm length, 70-nm diameter, and purity 95%.

The preparation method of a carbon reinforcement placed in the copper matrix consists of two main processes: sonication of compact materials and separation of dispersed forms. Both processes were carried out in liquids: MWNTs and RGO in an aqueous solution at a critical micellar concentration of Triton ×100; and graphene in pure ethanol (99.6% V). Sonication parameters: diameter of an ultrasonic probe tip, $\varnothing = 13$ mm; time, 4 min (pulsed: 1 s act/1 s pause); and total power, 576 J. The parameters of the separation process: 5000 rpm spin for 10 min. Figure 2 presents the morphology of the powders after the mixing process.

In the preliminary test, powders were axially pressed in a metallic die under the pressure of 200 MPa, and a "green body" was obtained. They were finally densified by the SPS method in a vacuum atmosphere (5×10^{-5} mbar) using the following parameters: sintering temperature = 950 °C, heating rate = 100 °C/min, holding time = 10 min, and pressure = 50 MPa. Pure copper was also sintered under the same conditions as a reference sample. The powders were sintered in a graphite die and, as a final product, we obtained cylindrical samples (diameter = $\varnothing 25$ mm, height = 5 mm). Density of the "green body" and samples after sintering were measured using a hydrostatic method.

Microstructural characterizations of the Cu-C powder mixtures and sintered composites were performed by means of scanning electron microscopy (SEM) using a Dual-Beam Auriga Zeiss microscope with an energy dispersive spectroscopy (EDS) detector (Bruker).

Dilatometric investigations were performed using a Netzsch DIL 402 C/4/G dilatometer. The temperature dependence of the relative linear expansion dL/L_o was measured, and the coefficient of thermal expansion (CTE), α (Alpha), was calculated as a function of the temperature according to Eq 1. The samples were heated up to the temperature of 1000 °C at a rate of 5 K/min in a protective pure argon atmosphere.

$$\alpha = \frac{\Delta l}{l_o \cdot \Delta T}, \tag{Eq 1}$$

where α is the thermal expansion coefficient, l_o is the initial length of the sample, Δl is the length increase, ΔT is the temperature increase.

Differential scanning calorimetry (DSC) measurements were performed by means of Netzsch DSC 404 C equipment. The samples were heated up to the temperature of 1000 °C at a rate of 5 K/min in a protective pure argon atmosphere.

The thermal diffusivity D was measured at room temperature by a laser flash method (LFA 427, Netzsch). The front face of the measured sample was homogeneously heated by an unfocused laser pulse. On the rear face of the sample, the temperature increase was measured as a function of time. The mathematical analysis of this temperature/time function allows for the determination of the thermal diffusivity D (Ref 19). The specific heat was evaluated based on the rule of mixture.

The experimental results of the thermal diffusivity and the calculated values of the specific heat were used to estimate the
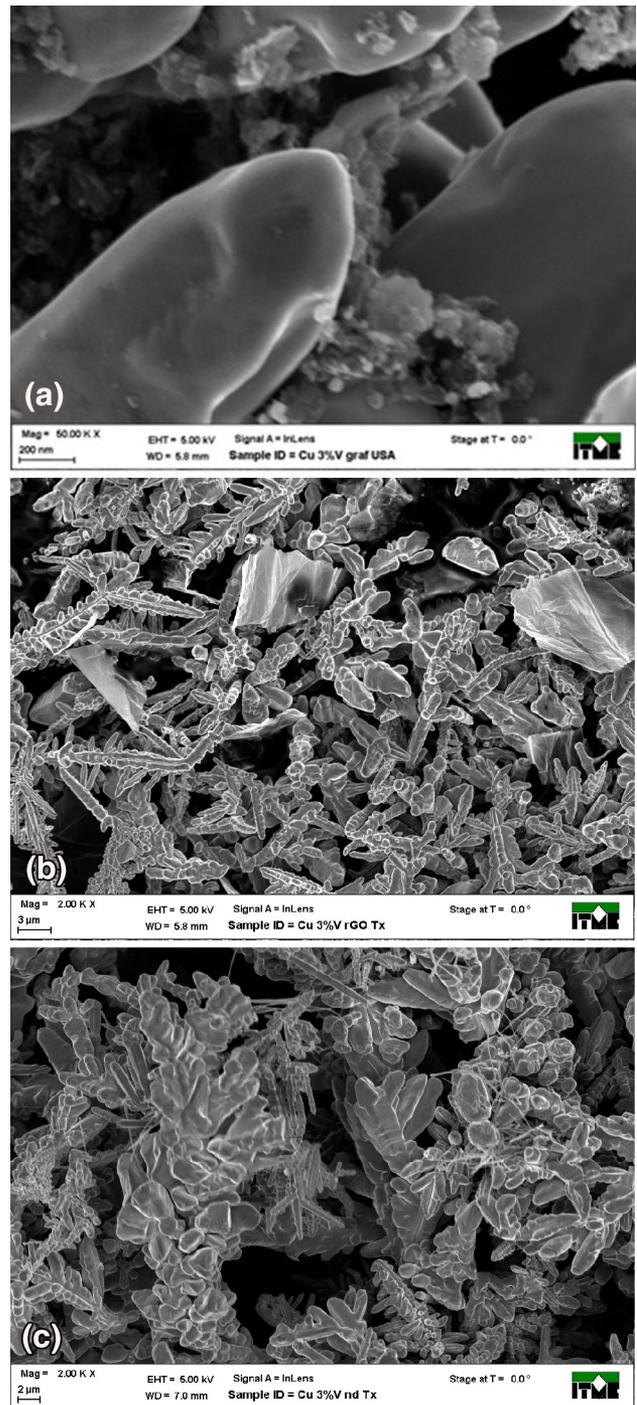

Fig. 2 SEM images of Cu-C powder mixtures with carbon in the form of (a) graphene, (b) graphene oxide, (c) nanotubes

thermal conductivity K. It can be determined from the following relation:

$$K = \rho \cdot c_p \cdot D, \tag{Eq 2}$$

where K is the thermal conductivity in W/mK, ρ is the density in g/cm^3, c_p is the specific heat in J/gK, and D is the diffusivity in mm^2/s.

3. Results and Discussion

Table 1 presents the results of density measurements performed for the obtained Cu-graphene composite materials. Theoretical density of the composites was defined for the assumed volume contents, using the density of carbon nanoforms $\rho_C = 1.22$ g/cm^3 and the density of copper $\rho_{Cu} = 8.89$ g/cm^3. Based on these data, the theoretical density ($\rho_{teor} = 8.71$ g/cm^3) of Cu-3%C was estimated.

The measurements show a high relative density for the materials (at least 99% of theoretical density value). There are no significant differences in density for various carbon forms used as the reinforcement.

The SEM observation of the microstructure of the Cu-C composites revealed that the carbon phase is quite evenly distributed in the entire volume of the material. Exemplary images of Cu-C composite structures are presented in Fig. 3, 4, and 5.

All images presented in Fig. 3, 4, and 5 were obtained from the cross sections of the samples produced in SPS processes. The cross sections of both Cu/RGO (Fig. 3a and b) and Cu/MWNT (Fig. 4a) composites clearly show the pores of the copper matrix, having a circular cross-sectional shape. No pores of the matrix are registered in SEM images of the Cu/GNP composite (Fig. 5a). Carbon forms built in the copper matrix have some distinguishing features. They are a derivative of the morphology of carbon structures and their size. The average flake size for RGO forms is one order of magnitude larger than for copper powder particles. In addition, the RGO structures are multilayered (Fig. 3b). The size of the RGO structures and their composition inhibit both densification and sintering of the composite material. The entire mass flow mechanism in the sintering process takes place around the RGO structure, especially as carbon and copper practically do not react together. That is why, deep pore slots appear around large RGO objects (Fig. 3b). Well-dispersed individual nanotubes, observed in each gap left after the detachment of Cu grains (Fig. 4a) in the case of low-resolution SEM, do not show porosity at the MWNT/Cu boundaries. With higher SEM resolution, nanopores are revealed on the lateral surface of nanotubes (Fig. 4b). In the process of sintering, the length of nanotubes close to the diameter of matrix particles leads to revealing only nanopores resulting from there being no Cu-C interaction. The average flake size of GNP after dispersion and centrifugation processes equals 0.7 μm. It is significantly lower than the diameter of copper matrix particles, thus facilitating densification and sintering processes of this composite. Moreover, GPN objects are composed of a few graphene layers on average. For this reason, SEM observation employing the InLens technique did not show clearly the coating of copper with GNP particles (Fig. 5a). On the other hand, in the case of the ESB/SEM technique (Fig. 5b), dispersed but homogeneous
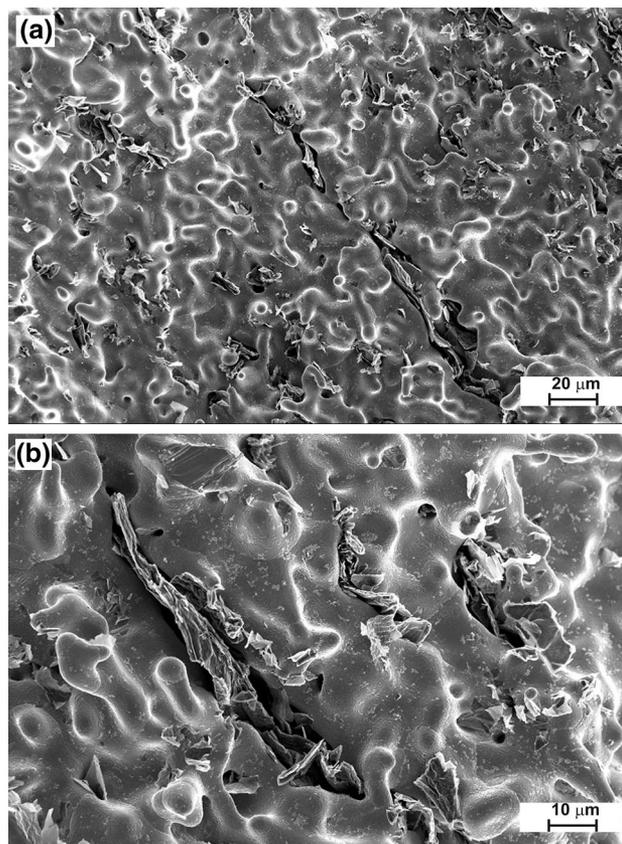

Fig. 3 SEM images of Cu-RGO composite material

coating of copper with GNP particles is observed (dark spots in Fig. 5b).

Measurement results of thermal diffusivity of Cu-C composites and estimated results of conductivity as a function of the temperature of these materials are presented in Fig. 6.

The measured thermal conductivity values of the composites, with a copper matrix doped with various forms of carbon in 3 vol.%, range between 330 and 370 W/mK. The results obtained at 50 °C are lower than both the literature data (theoretical thermal conductivity of pure copper is around 400 W/mK) and the measurement results of a reference sample of pure copper sintered using the SPS technique (about 380 W/mK). The highest thermal conductivity of Cu-C composites was achieved when employing carbon in the form of graphene flakes (366 W/mK), whereas the lowest was reached in the case of RGO (330 W/mK). The presence of oxygen significantly reduces heat transport properties in the crystal lattice of the graphene structure. It is well known that graphene as an anisotropic material is characterized by particularly high thermal conductivity in the direction of atomic rings. On the

Table 1 Density measurements performed for the obtained Cu-graphene composite materials

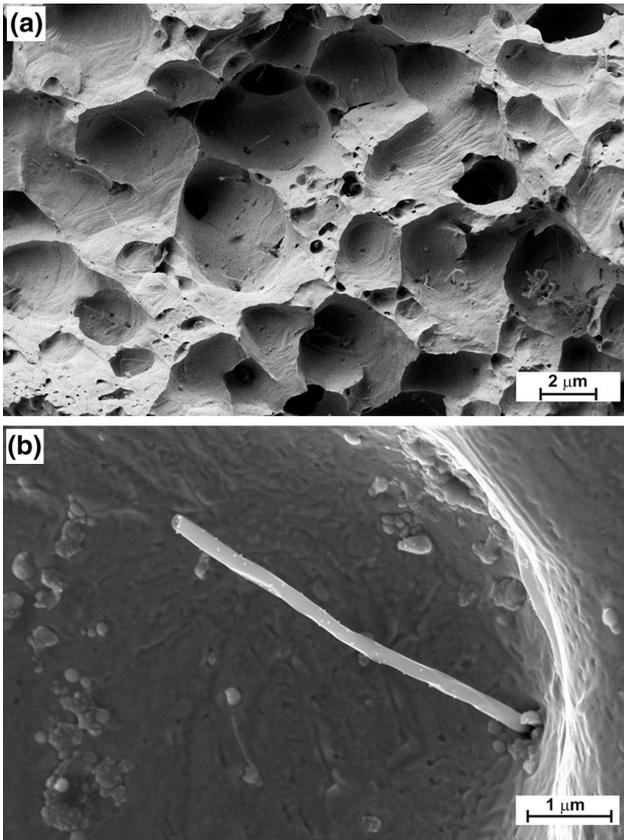| Materials	"Green body" density, g/cm^3	Measured density after sintering, g/cm^3	Relative density, %
Cu-3% RGO	6.25	8.66	99.4
Cu-3% MWNT	6.20	8.65	99.3
Cu-3% GNP	6.45	8.69	99.7

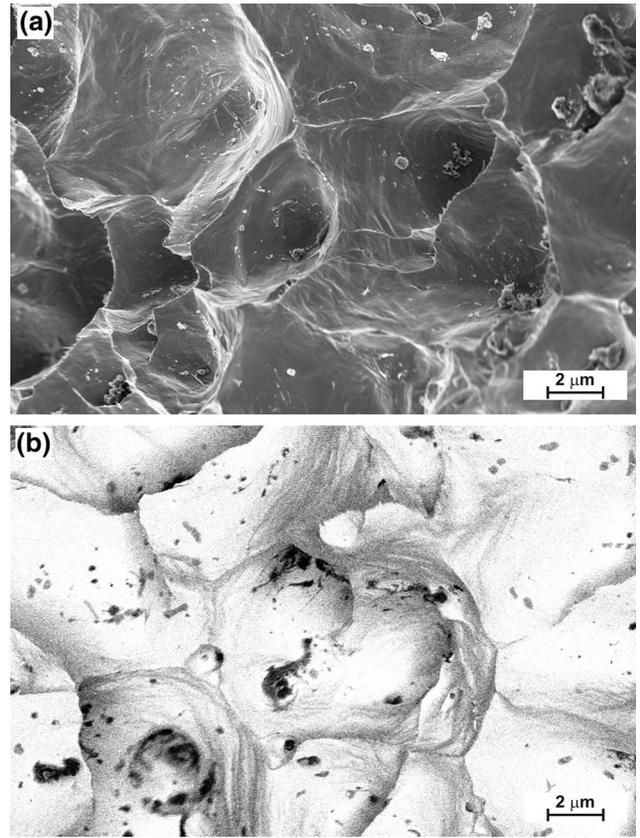Fig. 4   SEM images of Cu-MWNT composite material

Fig. 5   SEM images of Cu-GNP composite material

other hand, the location of graphene layers in the volumetric structure of the composite is random, and therefore in the majority of instances, heat does not flow through the graphene phase toward their top conduction. This does not have the visible effect of improving the thermal conductivity of the composite material containing graphene. Another factor reducing heat transport capacity of composites is the presence of pores in the structure of the material. Even though their quantity is not substantial and oscillates at the level below 1% depending on the applied carbon form, it undoubtedly is a barrier to the heat flux. The location of pores among individual graphene flakes and the formation of carbon phase clusters are also disadvantageous from the point of view of thermal conduction. As was stated in Ref 20, the size of pores plays a detrimental role in the heat conductivity of materials. Materials having a structure with a great number of fine pores conduct heat in a better manner than materials with a lower total number of bigger pores. In the case of Cu composites with nanotubes, the number and size of phonon-scattering centers have a less destructive influence on the heat flux than for composites doped with RGO. It was also found that the thermal conductivity values for all analyzed samples are decreased when the temperature is raised. This phenomenon is typical of the majority of metallic materials and is caused by the increased scattering of phonon carriers in the crystal lattice, observed when raising the temperature.

Figure 7 presents linear expansion curves of Cu-C composite materials, Cu (SPS), and Cu electrolytic measured during the first heating (1st run) and reheating (2nd run) to a temperature of 1000 °C.

Thermal expansion of the tested samples in the approximate temperature range of 300-800 °C is greater than the thermal expansion of pure electrolytic copper (Cu). The same material subjected to repeated heating has a very low thermal expansion, less than pure electrolytic copper. It means that the heat treatment involving heating to a high temperature leads to irreversible changes of the structure. DSC studies may be helpful in qualitative interpretation of measurement results of dilatometric investigations. Figure 8(a), (b) and 9(a), (b) show examples of DSC and CTE curves of the 1st and 2nd runs of Cu(SPS) and Cu-GNP composite materials, respectively.

DSC curves (1st run) show the presence of two thermal effects—endothermic in the temperature range of approx. 300-800 °C and exothermic at the higher temperature. The difference between the DSC curves (1-2) demonstrates that the first endothermic and irreversible effect corresponds to a significant increase in the volume (Fig. 7a), and the second exothermic and reversible can be ascribed to final decrease of volume.

Composite samples, due to lack of solubility of carbon in copper, do not show phase transitions or chemical reactions (e.g., oxidation). All the recorded changes in the dilatometric curves are mechanical changes and are associated with the consolidation process of composites. Lower-temperature dimensional changes accompanied by irreversible endothermic heat effect are probably related to the formation of stresses that may lead to permanent deformation of the matrix and increase
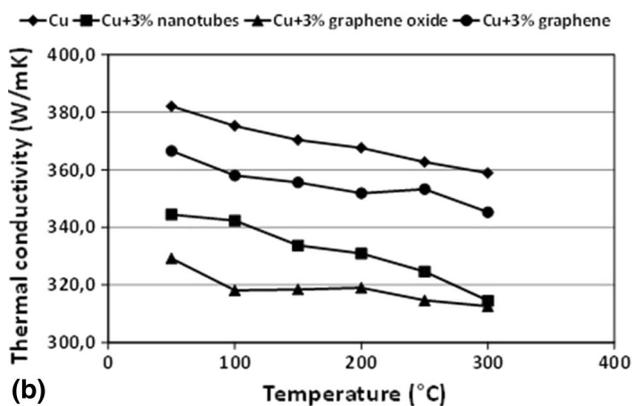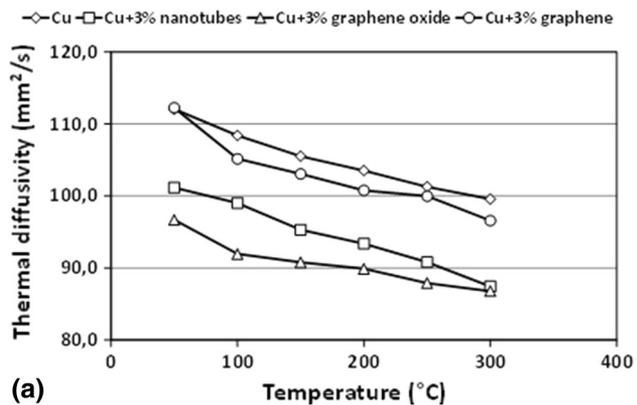
Fig. 6 Temperature dependence of (a) thermal diffusivity, (b) thermal conductivity of Cu-C composite materials
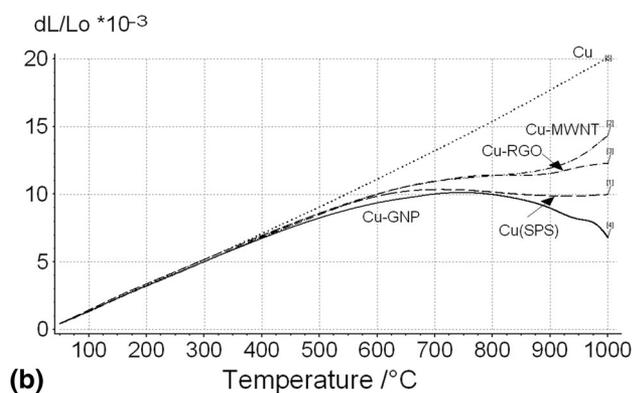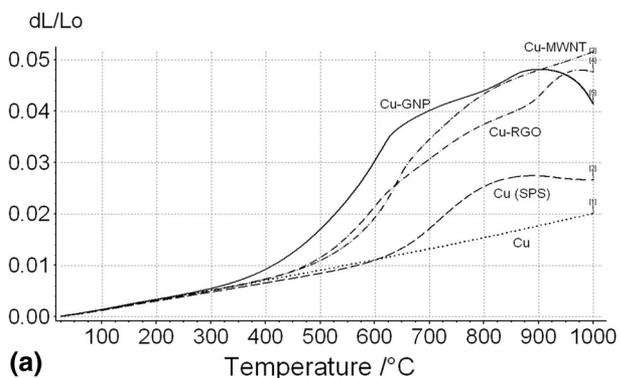

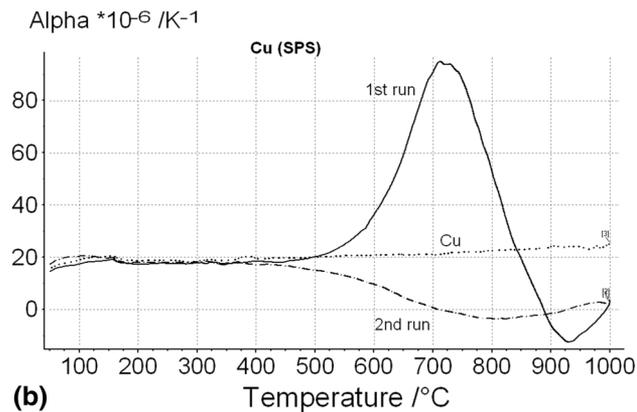**Fig. 7** Linear expansion curves of Cu-C composites—(a) after 1st heating, (b) after 2nd heating
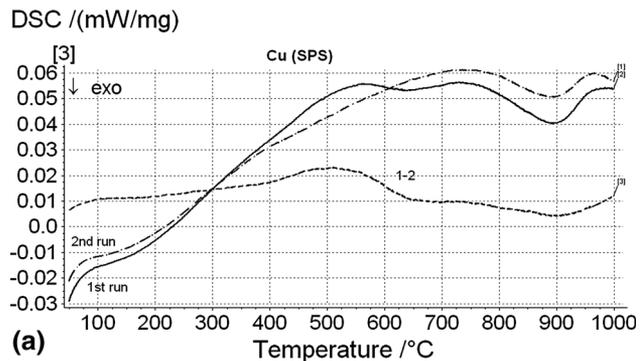

Fig. 8 Exemplary measuring curves of Cu (SPS)—(a) DSC, (b) CTE
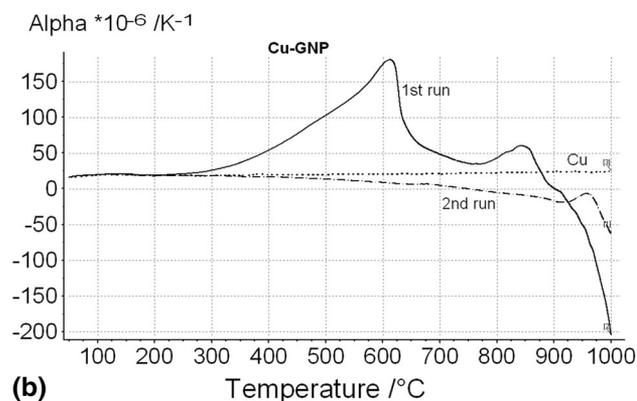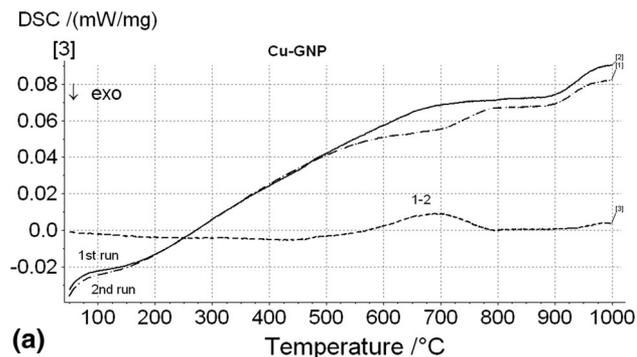

Fig. 9 Exemplary measuring curves of Cu-GNP composite—(a) DSC, (b) CTE

the volume of the composite. These stresses are caused by the differences in the thermal expansion curves of the copper and graphite matrices. Recrystallization and grain growth of the matrix characterized by exothermic effects may be also involved in this process. Final high-temperature contraction can be related to the presence of voids and pores in the composite structure.

4. Conclusions

This paper presents the results of experimental studies concerning the manufacture of Cu-C (multiwall carbon nanotubes (MWNTs), graphene nanopowder (GNP), or thermally reduced graphene oxide (RGO) composite materials and characterizations of their thermal properties, which are of crucial importance when being used in heat-dissipating systems. The technological conditions allowing one to obtain almost fully dense composite materials were developed using the SPS method. The best results from the point of view of their application to heat dissipation—the lowest (versus copper) CTE—were obtained for the composites containing GNP, after preheating to ca 800 °C. It was found that comparatively lower thermal conductivity values obtained for Cu-C composites (versus copper) are generated due to (i) the residual oxygen content and (ii) graphene anisotropic properties (extremely different values of thermal conductivity parallel and perpendicular to the surface of the used carbon forms). The presence of various forms of graphene in composites and the processes of consolidation, which are the source of adverse but thermally unstable dilatometric effects, and the explanation of these with the aim to remove them without loss of good thermal conductivity, require further study.

Acknowledgments

Open Access

References

1. M. Sakamoto, D. Welch, J. Endriz, D. Scifres, and W. Streifer, 76 W cw Monolithic Laser Diode Arrays, *Appl. Phys. Lett.*, 1989, **54**(23), p 2299–2300
2. D.D.L. Chung, Materials for Thermal Conduction, *Appl. Therm. Eng.*, 2001, **21**, p 1593–1605
3. A. Strojny-Nedza and K. Pietrzak, Processing, Microstructure and Properties of Different Method Obtained Cu-Al$_2$O$_3$ Composites, *Arch. Metall. Mater.*, 2014, **59**(4), p 1301–1306
4. G. CelebiEfe, S. Zeytin, and C. Bindal, The Effect of SiC Particle Size on the Properties of Cu-SiC Composites, *Mater. Des.*, 2012, **36**, p 633–639
5. M. Chmielewski and W. Weglewski, Comparison of Experimental and Modelling Results of Thermal Properties in Cu-AlN Composite Materials, *Bull. Pol. Acad. Sci. Tech.*, 2013, **61**(2), p 507–514
6. M. Chedru, J. Vicens, J.L. Chermant, and B.L. Mordike, Aluminium-Aluminium Nitride Composites Fabricated by Melt Infiltration Under Pressure, *J. Microsc.*, 1999, **196**(2), p 103–112
7. K.M. Lee, D.K. Oh, W.S. Choi, T. Weissgarber, and B. Kieback, Thermomechanical Properties of AlN-Cu Composite Materials Prepared by Solid State Processing, *J. Alloys Compd.*, 2007, **434–435**, p 375–377
8. L.J. Huang, L. Geng, and H.-X. Peng, Microstructurally Inhomogeneous Composites: Is a Homogeneous Reinforcement Distribution Optimal?, *Prog. Mater. Sci.*, 2015, **71**, p 93–168
9. T. Wejrzanowski, M. Grybczuk, M. Wasiluk, and K.J. Kurzydlowski, Heat Transfer Through Metal-Graphene Interfaces, *AIP Adv*, 2015, **5**, p 077142
10. J. Wang, Z. Li, G. Fan, H. Pan, Z. Chen, and D. Zhang, Reinforcement with Graphene Nanosheets in Aluminum Matrix Composites, *Scr. Mater.*, 2012, **66**(8), p 594–597
11. M. Popov, M. Kyotani, R.J. Nemanich, and Y. Koga, Superhard Phase Composed of Single-Wall Carbon Nanotubes, *Phys. Rev. B*, 2002, **65**(3), p 033408
12. S. Sinha, S. Barjami, G. Iannacchione, A. Schwab, and G. Muench, Off-Axis Thermal Properties of Carbon Nanotube Films, *J. Nanopart. Res.*, 2005, **7**(6), p 651–657
13. E. Thostenson, C. Li, and C.T. Chou, Nanocomposites in Context, *Compos. Sci. Technol.*, 2005, **65**(3–4), p 491–516
14. S.F. Moustafa, S.A. El-Badry, A.M. Sanad, and B. Kieback, Friction and Wear of Copper-Graphite Composites Made with Cu-Coated and Uncoated Graphite Powders, *Wear*, 2002, **253**, p 699–710
15. X. Jincheng, Y. Hui, L. Xiaolong, and Y. Hua, Effects of Some Factors on the Tribological Properties of the Short Carbon Fiber-Reinforced Copper Composite, *Mater. Des.*, 2004, **25**, p 489–493
16. S. Stankovich, D.A. Dikin, G.H.B. Dommett, K.M. Kohlhass, E.J. Zimney, E.A. Stach, R.D. Piner, S.T. Nguyen, and R.S. Ruoff, Graphene-Based Composite Materials, *Nature*, 2006, **442**(7100), p 282–286
17. A.D. Moghadam, E. Omrani, P.L. Menezes, and P.K. Rohatgi, Mechanical and Tribological Properties of Self-lubricating Metal Matrix Nanocomposites Reinforced by Carbon Nanotubes (CNTs) and Graphene—A Review, *Compos. Part B Eng.*, 2015, **77**, p 402–420
18. M. Tokita, Mechanism of Spark Plasma Sintering, *J. Soc. Powder Technol. Jpn.*, 1993, **30**, p 790–804
19. S. Min, J. Blumm, and A. Lindemann, A New Laser Flash Method for Measurement of the Thermophysical Properties, *Thermochim. Acta*, 2007, **455**, p 46–49
20. C. Vincent, J.F. Silvian, J.M. Heintz, and N. Chandra, Effect of Porosity on the Thermal Conductivity of Copper Processed by Powder Metallurgy, *J. Phys. Chem. Solids*, 2012, **73**, p 499–504